



The effect of inter-cluster interactions on the structure of colloidal clusters

Alex Malins^a, Stephen R. Williams^b, Jens Eggers^c, Hajime Tanaka^d, C. Patrick Royall^{e,*}

^a Bristol Centre for Complexity Science, School of Chemistry, University of Bristol, Bristol, BS8 1TS, UK

^b Research School of Chemistry, The Australian National University, Canberra, ACT 0200, Australia

^c School of Mathematics, University of Bristol, University Walk, Bristol, BS8 1TW, UK

^d Institute of Industrial Science, University of Tokyo, Meguro-ku, Tokyo 153-8505, Japan

^e School of Chemistry, University of Bristol, Bristol, BS8 1TS, UK

ARTICLE INFO

Article history:

Received 16 April 2010

Received in revised form 10 August 2010

Available online 9 September 2010

Keywords:

Colloids;

Clusters;

Brownian dynamics;

Liquids

ABSTRACT

Colloidal systems present exciting opportunities to study clusters. Unlike atomic clusters, which are frequently produced at extremely low density, colloidal clusters may interact with one another. Here we consider the effect of such interactions on the intra-cluster structure in simulations of colloidal cluster fluids. A sufficient increase in density leads to a higher population of clusters in the ground state. In other words, inter-cluster interactions perturb the intra-cluster behaviour, such that each cluster may no longer be considered as an isolated system. Conversely, for dilute, weakly interacting cluster fluids little dependence on colloid concentration is observed, and we thus argue that it is reasonable to treat each cluster as an isolated system.

© 2010 Elsevier B.V. All rights reserved.

1. Introduction

Clusters are a distinct state of matter which exhibit different structural ordering and phase behaviour, relative to bulk materials [1]. Of particular relevance to, for example, many biological systems such as viruses, is their tendency to exhibit five-fold symmetry such as icosahedra and decahedra [2]. Recently there has been a surge of interest in clusters formed in colloidal systems [3–13], leading to the development of ‘colloidal molecules’ [4,9,12,14,15]. These may in turn provide novel functionalised materials [4,9,10,12,14,15]. In addition to this technological relevance, the visualisation of colloidal clusters allows direct access to their free energy landscape [16].

Part of the attraction of studying colloidal dispersions is that, although in principle they are rather complex multicomponent systems, the spatial and dynamic asymmetry between the colloidal particles (10 nm–1 μm) and smaller molecular and ionic species has led to schemes where the smaller components are formally integrated out [17]. This leads to a one-component picture, where only the effective colloid–colloid interactions need be considered.

Given that the structure of ground state clusters of simple liquid models is known, along with local energy minima [2], it seems natural to investigate the prevalence of such structures in colloidal systems, in particular those with depletion attractions such as colloid–polymer mixtures where, at fixed real temperature, an effective temperature may be interpreted as the inverse of the attraction strength between the colloids. These colloidal systems exhibit similar [18–20] though

not identical [19,21] structures to clusters of simple liquid models. In general, as the (effective) temperature is reduced, we expect more clusters in the ground state, unless kinetic frustration comes into play.

Unlike atomic clusters, which are often considered in isolation, colloidal clusters may themselves form fluids [5,6]. Colloidal cluster fluids are found in systems with competing interactions with short-ranged attractions and long-ranged repulsions [5,6]. The attractions drive clustering while the repulsions prevent aggregation and phase separation, leading to a characteristic cluster size [22]. At sufficient concentration, these cluster fluids form gels [6,23–25], while for sufficiently strong repulsions, the cluster fluid can undergo dynamical arrest [26,27] or crystallisation [28]. Furthermore, the separation in length- and time-scales allows us to treat the system in a hierarchical manner. For example, dynamical arrest *within* clusters [29] and of a fluid comprised of clusters [26,27] can in general be decoupled. This hierarchy means that one may consider each cluster as an isolated system [30]. Alternatively, one may operate at the cluster–cluster level [31]. Here instead we consider the influence of the *inter*-cluster interactions on the *intra*-cluster behaviour. In other words, how is the free energy landscape of a given cluster perturbed by its neighbours?

In a recent experimental study on a cluster fluid [30], we observed that a rather small number of clusters were found in the expected ground state, around 20%. However, after a careful mapping of experimental parameters to conventional spherically symmetric interactions, Brownian dynamics simulations showed that isolated clusters reached their ground state, unless geometric frustration led to ergodicity breaking for deep quenches [29].

Here we consider an experimentally relevant set of conditions [30] and use Brownian dynamics simulations to investigate the effects of inter-cluster interactions on the intra-cluster behaviour. In particular

* Corresponding author.

E-mail address: paddy.royall@bristol.ac.uk (C.P. Royall).

we consider the population of clusters in the ground state. Our system is characterised by the colloid packing fraction ϕ , the strength of the attractive interaction $\beta\epsilon_M$ and the strength of the repulsion $\beta\epsilon_Y$, where $\beta = \frac{1}{k_B T}$, k_B is the Boltzmann constant and T is the temperature. We first determine the range of parameters that correspond to a cluster fluid, before investigating the effect that varying these parameters has on the intra-cluster structure.

2. Simulation details and model

Although a great many improvements have since been made [32,33], the theory of Asakura and Oosawa (AO) [34] is generally accepted to capture the essential behaviour of polymer-induced depletion attractions between colloids. This AO model ascribes an effective pair interaction between two colloidal hard spheres in a solution of ideal polymers. However, the hard core of the AO potential leads to difficulties with Brownian dynamics simulations. The Morse potential is a variable range spherically symmetric attractive interaction, and reads

$$\beta u_M(r) = \beta\epsilon_M e^{\rho_0(\sigma-r)} \left(e^{\rho_0(\sigma-r)} - 2 \right), \quad (1)$$

where ρ_0 is a range parameter, $\beta\epsilon_M$ is the potential well depth and σ is the diameter.

Under the right conditions, this produces similar behaviour to the Asakura–Oosawa model [35]. Here we follow our previous work and set $\rho_0 = 33.06$ and vary the potential well depth $\beta\epsilon_M$. This mimics the addition of polymer in the experiments and corresponds to a short-ranged attraction length of ≈ 0.22 [29]. We used weakly charged colloids to suppress aggregation. Under some circumstances, one can treat the colloid–colloid electrostatic repulsion with a Yukawa form

$$\beta u_Y(r) = \beta\epsilon_Y \frac{\exp(-\kappa(r-\sigma))}{r/\sigma}, \quad (2)$$

where κ is the inverse Debye screening length. The contact potential is given by

$$\beta\epsilon_Y = \frac{Z^2}{(1 + \kappa\sigma/2)^2} \frac{l_B}{\sigma}, \quad (3)$$

where Z is the colloid charge and l_B is the Bjerrum length. We use the experimentally relevant value for the inverse Debye length $\kappa\sigma = 0.5$ and likewise consider two values for the contact potential of the Yukawa repulsion $\beta\epsilon_Y = 1, 3$ [30]. In the experimental system we seek to model, van der Waals attractions are largely absent. Colloids have a hard core, which is often added to Eq. (2). Here, however, the Morse potential provides a slightly softened core, so we consider the combined potential $\beta u_M + \beta u_Y$ in the simulations.

For the simulations we use a standard Brownian dynamics simulation scheme [36]. The scheme generates a discrete coordinate trajectory \mathbf{r}_i as follows

$$\mathbf{r}_i(t + \delta t) = \mathbf{r}_i(t) + \frac{D}{k_B T} \sum_{j=1, j \neq i}^N \mathbf{F}_{ij}(t) \delta t + \delta \mathbf{r}_i^G, \quad (4)$$

where δt is the simulation time-step, D is the diffusion constant and N is the total number of particles. The colloids respond to the pairwise interactions \mathbf{F}_{ij} and the solvent-induced thermal fluctuations $\delta \mathbf{r}_i^G$ are treated as a Gaussian noise with the variance given by the fluctuation–dissipation theorem. Treatment of the hydrodynamic interaction between colloids is not included in the simulations.

For each state point of $\beta\epsilon_Y = \{1, 3\}$, $\phi = \{0.02, 0.05, 0.10\}$ and $\beta\epsilon_M = \{5, 6, 7, 8, 9, 10, 11, 12\}$ which span the range from monomer fluids to aggregates/gels, we perform 8 statistically independent simulations each of $N = 1000$ particles. Particles are initialized randomly subject to

a non-overlap constraint in a cubic box. Periodic boundary conditions for the box are implemented. The Morse potential (Eq. (1)) is truncated and shifted for $r > 1.5\sigma$, where the Morse potential is typically less than 10^{-6} . The electrostatic interactions are treated by adding a Yukawa repulsion term (Eq. (2)) for different values of $\beta\epsilon_Y$ as specified and this is also truncated and shifted for $r > 10.175\sigma$, where the potential is of the order 10^{-3} . We study the evolution of the system as the particles condense into small clusters under the influence of the Morse attractions, which are stabilised by the long range Yukawa charged repulsions.

We define the Brownian time as the time taken for a colloid to diffuse its own radius:

$$\tau_B = \frac{(\sigma/2)^2}{6D}. \quad (5)$$

In the simulations, $\tau_B \approx 711$ time units, while in the experiments $\tau_B \sim 9$ [30]. The time-step is $\delta t = 0.03$ simulation time units and all runs are equilibrated for 1.5×10^7 steps and run for further 1×10^7 steps. The simulation runs therefore correspond to approximately 1000 Brownian times or around 1 h, a timescale certainly comparable to experimental work.

We identify two particles as bonded if the separation of the particle centres is less than 1.25σ [29]. Having identified the bond network, we use the Topological Cluster Classification (TCC) to determine the nature of the cluster [37]. This analysis identifies all the shortest path three, four and five membered rings in the bond network, and identifies the clusters from these base units. We use the TCC to find clusters which are global energy minima of the Morse potential [21]. We denote the number of particles in a cluster by m and follow Doye et al. in terming the global energy minima clusters by the number of particles, the range of the potential and the point group symmetry of the cluster. The global energy minimum $m = 3, 4, 5, 6, 7$ clusters for the Morse potential with $\rho_0 = 33.06$ are 3A D_{3h} triangle, 4A T_d tetrahedron, 5A D_{3h} triangular bipyramid, 6A O_h octahedron, and 7A D_{5h} pentagonal bipyramid respectively and the structures are depicted in Fig. 5. For $m \leq 7$ there is only one global minimum for all ranges of the Morse potential. For more details, see [37].

3. Results

3.1. Phase diagram

Here we are interested in cluster fluids, however at low density and/or low attraction, the system is dominated by unbound particles which we term a monomer fluid (Fig. 1(a)) while at high density we find aggregation into much larger, often elongated [18,22] clusters and ultimately gelation (Fig. 1(c)) [6,23]. Between the aggregation/gel regime and the monomer fluid lies the cluster fluid seen in Fig. 1(b).

We begin our presentation of the results by determining those state points we consider to be cluster fluids. To do this, we analyse the cluster size distribution, as shown in Fig. 2. In the limit that $\beta\epsilon_M \rightarrow 0$ we expect a monomer fluid of isolated colloids as shown in Fig. 2(a) for weakly attracting systems $\beta\epsilon_Y = 1, \phi = 0.02$, $\beta\epsilon_M \sim 4$. We find a crossover to a system dominated by clusters at $\beta\epsilon_M \sim 7$. At higher interaction strengths, the number of monomers drops markedly, as the system moves towards larger clusters. As Fig. 2(a) shows, for moderate values of the attractive interaction $\beta\epsilon_M$, most clusters have a size $m \leq 10$. We take an arbitrary value of 50% to distinguish the three states in Fig. 1. In other words, we consider a system with more than half the particles as monomers to be a monomer fluid, and with more than half the particles in $m > 10$ aggregates to be either aggregated or gelled. Increasing colloid packing fraction $\phi = 0.1$ and Yukawa interaction strength $\beta\epsilon_Y = 3$ (Fig. 2(b)) leads to a somewhat different scenario. Here, we find clusters at all measured attraction strengths. Furthermore, for moderate interaction strengths, the distributions

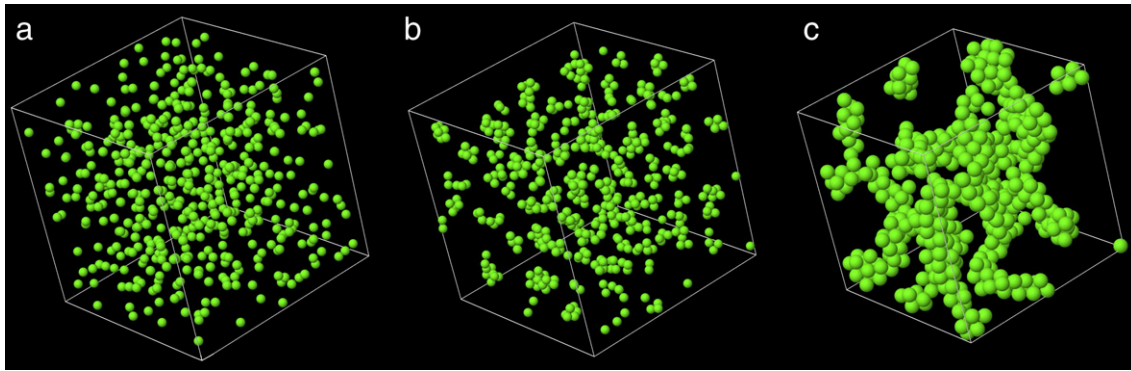


Fig. 1. Simulation snapshots of the three states seen (a) $\beta\epsilon_Y=3, \phi=0.02, \beta\epsilon_M=5$, monomer fluid where more than 50% of the particles are identified as monomers/unbonded, (b) $\beta\epsilon_Y=3, \phi=0.02, \beta\epsilon_M=9$, cluster fluid in which we are interested, and (c) $\beta\epsilon_Y=1, \phi=0.10, \beta\epsilon_M=12$, aggregate/gel where more than 50% of particles are identified in $m>10$ clusters.

seem rather flat, with a high incidence of large clusters, or aggregates. In fact no monomers or dimers are present for $\beta\epsilon_M>8$. Finding clusters at all interaction strengths is likely related to the increase in packing fraction to $\phi=0.1$ relative to Fig. 2(a). Colloids have less chance to avoid one another. Recall that the Yukawa repulsion is very long-ranged ($\kappa\sigma=0.5$). The mean interparticle separation $(6\phi/\pi)^{-1/3}$ at $\phi=0.1$ is 1.74σ , and the Yukawa repulsion varies only by $1.81k_B T$ between 1.74σ and contact, so particles readily approach one another. Note that this crossover away from monomers at higher $\beta\epsilon_M$ is in marked contrast to a number of experiments [5–7] which found an appreciable number of monomers even at high strengths of the attractive interaction.

Based on the cluster size distributions, we now determine phase diagrams following our criteria for monomer fluids, cluster fluids and aggregates/gels. These are shown in Fig. 3. The generic nature is similar to that found in the previous simulation [23] and experimental [6] work, of monomer fluids at low density and weak attractions, gels/aggregates at higher density/attraction and a cluster fluid in between. Our definitions lead to a crossover rather than an abrupt transition for both the monomer-cluster fluid and cluster fluid-aggregate/gel. The differences between Fig. 3(a) and (b) are reasonably understood in terms of the increase in the Yukawa repulsion, which inhibits clustering at the low colloid packing fraction ϕ we consider.

3.2. Inter-cluster interactions

Pair correlation functions are shown in Fig. 4. Fig. 4(a) is a low density $\phi=0.02$ $\beta\epsilon_Y=1.0$ $\beta\epsilon_M=6.0$ system, while for (b) $\phi=0.1$ $\beta\epsilon_Y=3.0$ $\beta\epsilon_M=7.0$. In both cases, the intra-cluster structure for $r<3\sigma$ shows strong peaks. The pair correlation functions also allow us to

comment on the strength of the cluster–cluster interactions. Fig. 4(b) shows a broad peak at $r\sim 4\sigma$, conversely at longer ranges in Fig. 4(a), $g(r)$ is almost flat. The peak in Fig. 4(b) indicates that these clusters exhibit strong correlations with their neighbours and are thus interacting with one another. Conversely, Fig. 4(a) is a weakly interacting system.

By thinking of the cluster fluid as a fluid of (polydisperse) Yukawa-like particles [31], we can gain some idea of the interaction between clusters. For the state point in Fig. 4(b), the mean cluster size is $\langle m \rangle \approx 8.75$. Typical cluster–cluster separations are given by the cluster–cluster peak i.e. $r_{CC} \sim 4\sigma$. If we consider clusters of average size at the typical separation, we have a cluster–cluster interaction (i.e. pair interaction) of $\beta U_{CC} = \langle m \rangle^2 \beta U_Y(r_{CC}) \approx 14$. Conversely, in the case of Fig. 4(a), there is a very weak peak around $r \approx 6.25\sigma$, $\langle m \rangle \approx 3.55$, which leads to a typical cluster–cluster interaction strength of $\beta U_Y(r_{CC}) \approx 0.15$. We can thus speak of weakly interacting (Fig. 4(a)) and strongly interacting (Fig. 4(b)) cluster fluids. We expect that a weakly interacting cluster fluid should show little change relative to isolated clusters, but that in a strongly interacting cluster fluid, the energy landscape of each cluster can be perturbed by its neighbours.

3.3. Cluster populations

In the cluster fluid, we treat each cluster individually, and measure its structure. In order to do this we identify the proportion of m -membered clusters which are in the ground state. We expect that, in the absence of geometric frustration (which is the case for $m<6$), the cluster population will be dominated by the ground state at sufficient attraction.

Our main results are given in Figs. 5 and 6. Here we see that, as expected, for $3 \leq m \leq 5$, all clusters at all state points are largely found in the ground state for sufficient values of $\beta\epsilon_M$. The case of $m=6$

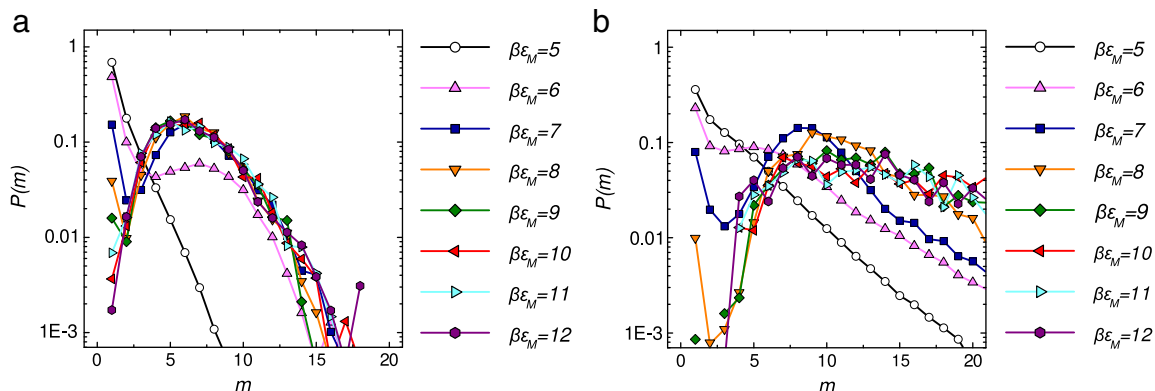


Fig. 2. Cluster size distributions. m denotes number of particles in a cluster and lines are different values of $\beta\epsilon_M$. (a) $\beta\epsilon_Y=1, \phi=0.02$, and (b) $\beta\epsilon_Y=3, \phi=0.1$.

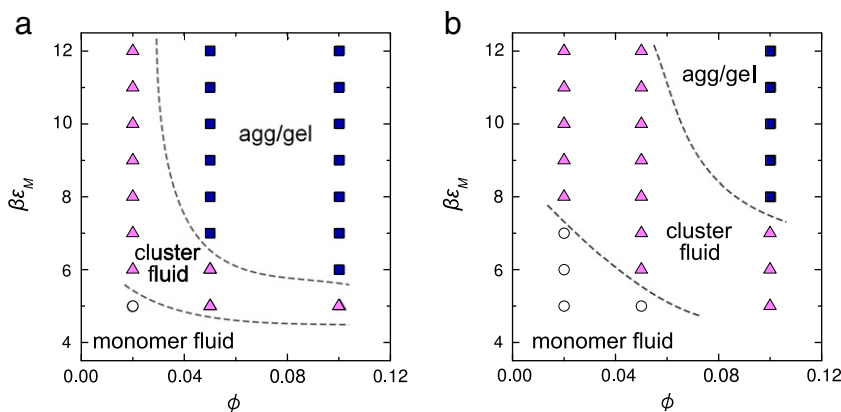


Fig. 3. Phase diagrams in the $\phi - \beta\epsilon_M$ plane. States are classified as monomer fluid, cluster fluid or aggregate/gel as defined in the text. The panels refer to different strengths of the Yukawa repulsion. Dashed lines are a guide to the eye. (a) $\beta\epsilon_Y = 1.0$, and (b) $\beta\epsilon_Y = 3.0$.

(Figs. 5(d,e) and 6(d,e)) is somewhat different, as two structures, the 6Z C_{2v} and the 6A O_h octahedron compete. Both have the same number of near-neighbours. Without the Yukawa repulsions the difference in potential energy for our system is very small (of order 1 part in 1×10^8) [29], which slightly favours the 6A O_h octahedron. However symmetry and vibrational contributions to the free energy favour C_{2v} by a factor of around 30 [16] as we indeed see. Here, the inclusion of the Yukawa repulsions $\beta\epsilon_Y > 0$ means that 6Z C_{2v} is somewhat favoured energetically.

In the case of 7-membered clusters (Fig. 5(f)), the population of the global minimum 7A D_{5h} pentagonal bipyramid does not tend to unity. We showed this is due to ergodicity breaking at relatively deep quenches, such that geometric frustration can prevent access to the pentagonal bipyramid ground state [29]. For these relatively short simulation runs ($\tau = 400\tau_B$), once the attractive interaction strength exceeds $\beta\epsilon_M \sim 5.0$ the bond lifetime exceeds the simulation run time.

We now turn our attention to the role of increasing density for the $\beta\epsilon_Y = 3.0$ system (Fig. 5). We see a general trend of higher density promoting access to the ground state. This is particularly true for those clusters in which there is no geometric frustration limiting access to the ground state, 3A D_{3h} triangles, 4A T_d tetrahedra, 5A D_{3h} triangular bipyramids and 6Z C_{2v} . The effect of colloid packing fraction appears the strongest around $\beta\epsilon_M \sim 6$. For example, we find an order of magnitude increase in the 6Z C_{2v} population at $\beta\epsilon_M = 6.0$ upon increasing the packing fraction from $\phi = 0.05$ to $\phi = 0.1$ (Fig. 5(e)). For these clusters, the effect of raising the colloid concentration may thus be thought of as acting in a similar way to an increase in attraction $\beta\epsilon_M$. The 6A O_h octahedron population is around 1/30 that of the 6Z C_{2v} , which is consistent with simulations [29] and experiments [16] on isolated clusters. Compared to isolated systems [29], we see relatively few 7A D_{5h} pentagonal bipyramids.

In the case of weaker Yukawa repulsions (Fig. 6), our arguments above concerning ‘strongly’ and ‘weakly’ interacting cluster fluids would lead us to imagine that reducing the repulsions would lead to less inter-cluster interactions and less perturbation of the intra-cluster behaviour. This appears to be the case: compared to Fig. 5, the relatively weakly interacting clusters in Fig. 6 show less response to increasing the colloid packing fraction. In particular the more dilute $\phi = 0.02$ and 0.05 show little deviation from one another. This suggests that for these parameters, the cluster fluid approaches the dilute limit and behaves as a ‘cluster gas’. Note that the experimental system considered in [30] was close to $\phi = 0.02$, $\beta\epsilon_Y = 1.0$ i.e. ‘weakly interacting’.

4. Discussion

We have considered the effect of cluster–cluster interactions on the intra-cluster structure in the Brownian dynamics simulations of a cluster fluid. The overall behaviour is broadly similar to isolated clusters. That is to say, upon increasing the strength of the attraction clusters are able to reach their ground states, unless geometrically frustrated from doing so [29]. For weak cluster–cluster interactions around $0.15k_B T$ between individual clusters, the intra-cluster behaviour depends little upon density. We therefore conclude that weakly interacting colloidal cluster fluids at low density (such as $\phi = 0.02$, $\beta\epsilon_Y = 1$) may be reasonably treated as independent systems. Introducing a stronger coupling between the clusters such as increasing density leads to a higher population of clusters in the ground state for a given interaction strength. In other words, the energy landscape of each cluster is perturbed by its neighbours.

This may be qualitatively understood in terms of the repulsive Yukawa interactions between clusters. The pair interaction energy between clusters typically increases as the clusters approach one another upon raising the colloid packing fraction. These inter-cluster

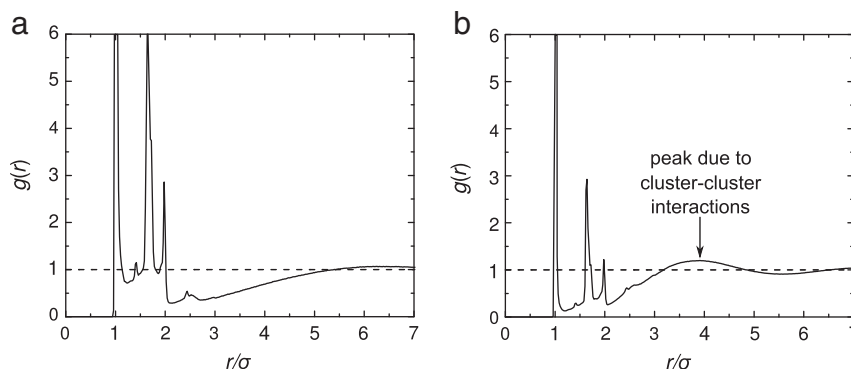


Fig. 4. Pair correlation functions in cluster fluids. (a) Weakly interacting cluster fluid, $\phi = 0.02$, $\beta\epsilon_Y = 1.0$, $\beta\epsilon_M = 6.0$. (b) Strongly interacting cluster fluid, $\phi = 0.1$, $\beta\epsilon_Y = 3.0$, $\beta\epsilon_M = 7.0$.

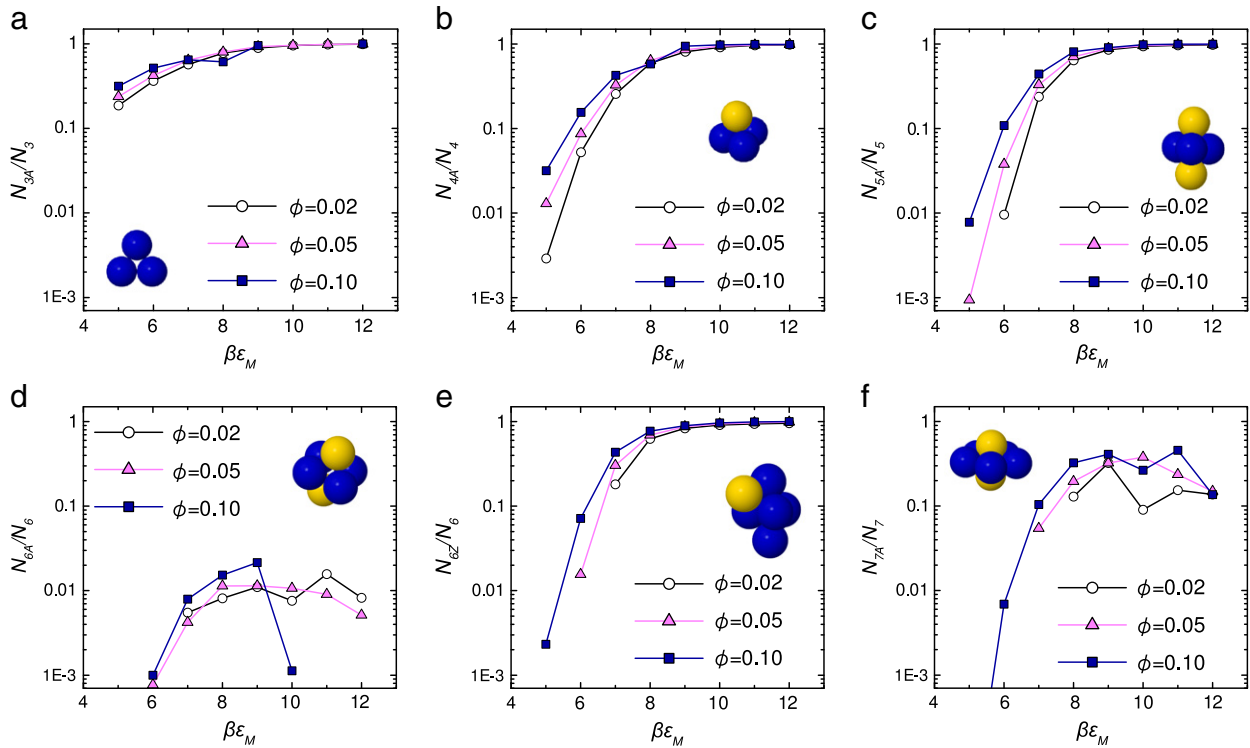


Fig. 5. Cluster populations of each cluster size $3 \leq m \leq 7$ as a function of the well depth of the attractive interaction $\beta\epsilon_M$. Here we fix $\beta\epsilon_V = 3$. We define cluster population by the ratio N_c/N_m where N_m and N_c are the total number of clusters of size m and the total number of clusters of type c (with m colloids) respectively. Symbols refer to colloid packing fraction, $\phi = 0.02$, circles, $\phi = 0.05$, triangles, $\phi = 0.10$, squares. The different plots corresponding to cluster structures (a) $3A D_{3h}$ triangles, (b) $4A T_d$ tetrahedra, (c) $5A D_{3h}$ triangular bipyramids, (d) $6Z C_{2v}$, (e) $6A O_h$ octahedra, and (f) $7A D_{5h}$ pentagonal bipyramids.

repulsions might be expected to favour ‘compact’ clusters. One example of ‘compact’ is a cluster which minimises its radius of gyration. For spheres, these are $3A D_{3h}$ triangles, $4A T_d$ tetrahedra

and $7A D_{5h}$ pentagonal bipyramids [38]. Therefore, increasing cluster-cluster repulsions can lead to similar behaviour as increasing the strength of attraction. This may be equivalent to noting that clusters of

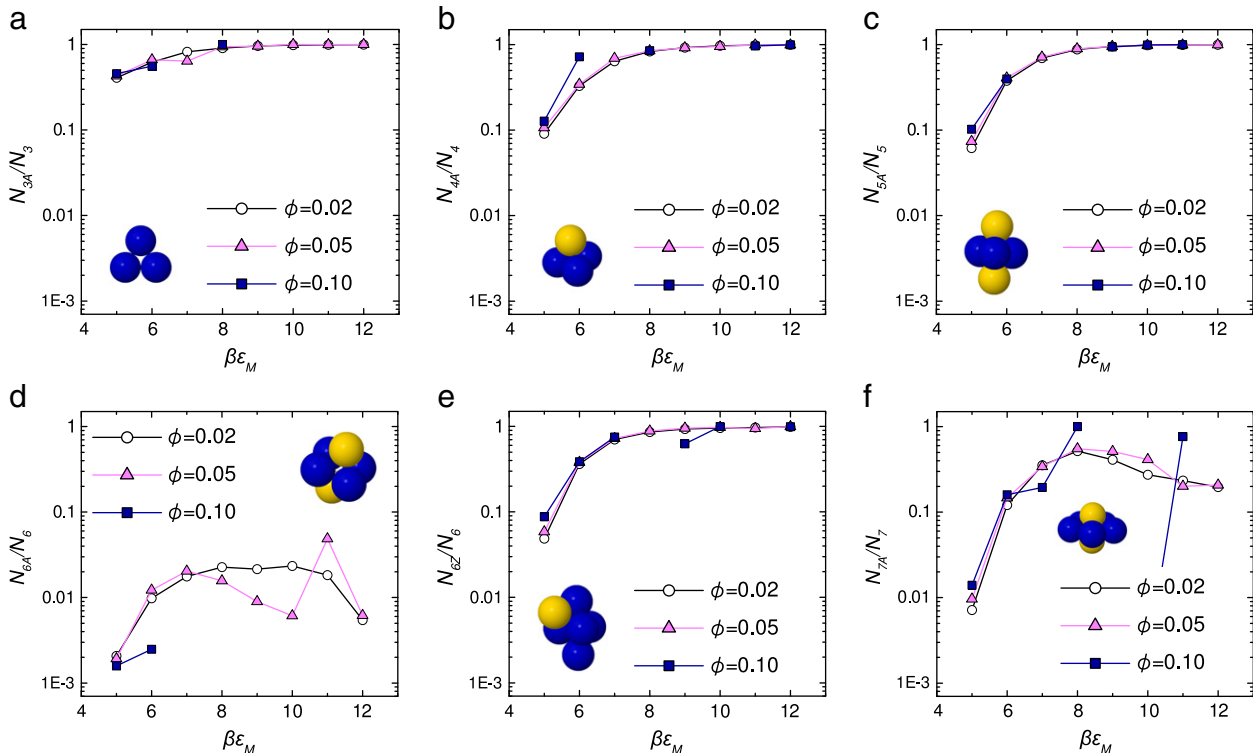


Fig. 6. Cluster populations for $\beta\epsilon_V = 1$. Symbols refer to colloid packing fraction, $\phi = 0.02$, circles, $\phi = 0.05$, triangles, $\phi = 0.10$, squares. The different plots corresponding to cluster structures (a) $3A D_{3h}$ triangles, (b) $4A T_d$ tetrahedra, (c) $5A D_{3h}$ triangular bipyramids, (d) $6Z C_{2v}$, (e) $6A O_h$ octahedra, and (f) $7A D_{5h}$ pentagonal bipyramids.

hard spheres which minimize the radius of gyration exhibit the same structures as for the ground states for particles with attractive interactions 3A D_{3h} triangles, 4A T_d tetrahedra, 5A D_{3h} triangular bipyramids, 6A O_h octahedra and 7A D_{5h} pentagonal bipyramids [4]. One interesting approach would be to take a system which forms markedly different clusters, such as 'patchy particles' which can be tailored to form less compact structures in the ground state [10]. The competition between compact clusters favoured by density and the less compact ground state clusters could then be investigated. In this system, there in fact may be some competition between 6Z C_{2v} (favoured in isolation) and the 6A O_h octahedron which is more compact.

It is important to note that, although we simulate on experimentally relevant time-scales, the cluster fluids we have studied here may not be truly at equilibrium. Colloidal cluster systems have been shown in simulation to form cluster crystals [28] or lanes [39], but this suggests a more uniform cluster size distribution than we find here. Therefore, even though our cluster–cluster interactions can reach $14k_B T$, the inherent polydispersity in the system prevents crystallisation. Systems with competing interactions often exhibit some form of structural ordering [40]. It is reasonable to suppose that much longer simulation runs than we have been able to perform here might result in a shift in the cluster size distribution to one which is more monodisperse. Moreover, state points at higher concentration might be expected to develop into columnar phases or lamellae with a clear periodicity [40,41]. We have not investigated the cluster dynamics in this system, but it is possible that there is a cluster glass region of the phase diagram.

According to the definitions we have used here, there is no sharp transition between cluster fluids and aggregates/gels. Increasing density/attractions leads to aggregation and gelation. However, locally in the gel we may expect the structure to resemble that of the clusters. This we indeed found in experiments on gelation without long-ranged repulsion [42]. With competing interactions, as is the case here, a crossover from a cluster glassy state to a gel has been seen [27], where gelation is interpreted as a percolation phenomenon. That study found little change in local structure upon gelation. Thus both arrested spinodal type gels without long-ranged repulsions [42,43] and those gels resulting from percolation in a system with competing interactions [6,24,27] may have a local structure dominated by a topology which follows that of isolated clusters.

5. Conclusions

The effect of cluster–cluster interactions on the intra-cluster structure of a model colloidal system has been studied. In the case of weak cluster–cluster interactions at low colloid concentration, the yield of structures is similar to if the clusters were isolated. This is the 'cluster gas' limit and interactions between clusters may be neglected. By increasing colloid density and/or increasing the strength of the Yukawa repulsion between colloids, cluster–cluster interactions become stronger and may no longer be neglected. Increasing either the density or the Yukawa repulsion causes a higher yield of ground state structures, showing that energy landscape of a cluster is perturbed by the presence of neighbouring clusters. The 'cluster fluid' cannot be approximated as an isolated system due to the presence of cluster–cluster interactions which perturb the intra-cluster structure.

Acknowledgements

CPR thanks the Royal Society for funding, AM acknowledges the support of EPSRC grant EP/5011214. This work was carried out using the computational facilities of the Advanced Computing Research Centre, University of Bristol – <http://www.bris.ac.uk/acrc/>.

References

- [1] F. Baretto, R. Ferrando, Structural properties of nanoclusters: energetic, thermodynamic, and kinetic effects, *Rev. Mod. Phys.* 77 (2005) 371–423.
- [2] D.J. Wales, *Energy Landscapes: Applications to Clusters, Biomolecules and Glasses*, Cambridge University Press, Cambridge, 2004.
- [3] P.N. Segre, V. Prasad, A.B. Schofield, D.A. Weitz, Glasslike kinetic arrest at the colloidal-gelation transition, *Phys. Rev. Lett.* 86 (2001) 6042–6045.
- [4] V.N. Manoharan, M.T. Elessor, D.J. Pine, Dense packing and symmetry in small clusters of microspheres, *Science* 301 (2003) 483–487.
- [5] A. Stradner, H. Sedgwick, F. Cardinaux, W.C.K. Poon, S.U. Egelhaaf, P. Schurtenberger, Equilibrium cluster formation in concentrated protein solutions and colloids, *Nature* 432 (2004) 492–495.
- [6] A.I. Campbell, V.J. Anderson, J.S. van Duijneveldt, P. Bartlett, Dynamical arrest in attractive colloids: the effect of long-range repulsion, *Phys. Rev. Lett.* 94 (2005) 208301.
- [7] H. Sedgwick, S.U. Egelhaaf, W.C.K. Poon, Clusters and gels in systems of sticky particles, *J. Phys. Condens. Matter* 16 (2004) S4913–S4922.
- [8] C.J. Dibble, M. Kogan, M.J. Solomon, Structure and dynamics of colloidal depletion gels: coincidence of transitions and heterogeneity, *Phys. Rev. E* 74 (2006) 041403.
- [9] S.C. Glotzer, M.J. Solomon, Anisotropy of building blocks and their assembly into complex structures, *Nat. Mater.* 6 (2007) 557–562.
- [10] A.W. Wilber, J.P.K. Doye, A.A. Louis, E.G. Noya, M.A. Miller, P. Wong, Reversible self-assembly of patchy particles into monodisperse clusters, *J. Chem. Phys.* 127 (2007) 085106.
- [11] D. Zerrouki, J. Baudry, D. Pine, P. Chaikin, J. Bibette, Chiral colloidal clusters, *Nature* 455 (2008) 380–382.
- [12] S.M. Anthony, M. Kim, S. Granick, Translation–rotation decoupling of colloidal clusters of various symmetries, *J. Chem. Phys.* 129 (2008) 244701.
- [13] P. Akcora, H. Liu, S.K. Kumar, J. Moll, Y. Li, B.C. Benicewicz, L.S. Schadler, L.S. Acehan, A.Z. Panagiotopoulos, V. Pryamitsyn, V. Ganesan, J. Ilavsky, P. Thiyagarajan, R.H. Colby, J.F. Douglas, Anisotropic self-assembly of spherical polymer-grafted nanoparticles, *Nat. Mater.* 8 (2009) 354–359.
- [14] Z. Zhang, A.S. Keys, T. Chen, S.C. Glotzer, Self-assembly of patchy particles into diamond structures through molecular mimicry, *Langmuir* 21 (2005) 11547–11551.
- [15] E.G. Noya, C. Vega, J.P.K. Doye, A.A. Louis, Phase diagram of model anisotropic particles with octahedral symmetry, *J. Phys. Chem.* 127 (2007) 054501.
- [16] G. Meng, N. Arkus, M.P. Brenner, V.N. Manoharan, The free-energy landscape of clusters of attractive hard spheres, *Science* 327 (2010) 560–563.
- [17] C.N. Likos, Effective interactions in soft condensed matter physics, *Phys. Rep.* 348 (2001) 267–439.
- [18] S. Mossa, F. Sciortino, P. Tartaglia, E. Zaccarelli, Ground-state clusters for short-range attractive and long-range repulsive potentials, *Langmuir* 20 (2004) 10756–10763.
- [19] N. Arkus, V.N. Manoharan, M.P. Brenner, Minimal energy clusters of hard spheres with short range attractions, *Phys. Rev. Lett.* 118 (2009) 118303.
- [20] D.J. Wales, Energy landscapes of clusters bound by short-ranged potentials, *ChemPhysChem* 11 (2010) 2491–2494.
- [21] J.P.K. Doye, D.J. Wales, R.S. Berry, The effect of the range of the potential on the structures of clusters, *J. Chem. Phys.* 103 (1995) 4234–4249.
- [22] J. Groenewold, W.K. Kegel, Anomalously large equilibrium clusters of colloids, *J. Phys. Chem. B* 105 (2001) 11702–11709.
- [23] F. Sciortino, P. Tartaglia, E. Zaccarelli, One-dimensional cluster growth and branching gels in colloidal systems with short-range depletion attraction and screened electrostatic repulsion, *J. Phys. Chem. B* 109 (2005) 21942–21953.
- [24] E. Zaccarelli, Colloidal gels: equilibrium and non-equilibrium routes, *J. Phys., Condens. Matter* 19 (2007) 323101.
- [25] K. Kroy, M.E. Cates, W.C.K. Poon, Cluster mode-coupling approach to weak gelation in attractive colloids, *Phys. Rev. Lett.* 92 (2004) 148302.
- [26] J.C. Fernandez Toledano, F. Sciortino, E. Zaccarelli, Colloidal systems with competing interactions: from an arrested repulsive cluster phase to a gel, *Soft Matter* 5 (2009) 2390–2398.
- [27] C.L. Klíx, C.P. Royall, H. Tanaka, Structural and dynamical features of multiple metastable glassy states in a colloidal system with competing interactions, arXiv: 1002.1502v1 [cond-mat.soft] (2010).
- [28] B.M. Mladek, D. Gottwald, G. Kahl, M. Neumann, C.N. Likos, Formation of polymorphic cluster phases for a class of models of purely repulsive soft spheres, *Phys. Rev. Lett.* 96 (2006) 045701.
- [29] A. Malins, S.R. Williams, J. Eggers, H. Tanaka, C.P. Royall, Geometric frustration in small colloidal clusters, *J. Phys., Condens. Matter* 21 (2009) 425103.
- [30] C.L. Klíx, K. Murata, H. Tanaka, S.R. Williams, A. Malins, C.P. Royall, The role of weak charging in metastable colloidal clusters, arXiv: 0905.3393v1 [cond-mat.soft] (2009).
- [31] F. Sciortino, S. Mossa, E. Zaccarelli, P. Tartaglia, Equilibrium cluster phases and low-density arrested disordered states: the role of short-range attraction and long-range repulsion, *Phys. Rev. Lett.* 93 (2004) 055701.
- [32] K.S. Schweizer, M. Fuchs, Structure of colloid–polymer suspensions, *J. Phys., Condens. Matter* 14 (2002) R239–R269.
- [33] R. Tuinier, J. Riegger, C.G. de Kruif, Depletion-induced phase separation in colloid–polymer mixtures, *Adv. Colloid Interface Sci.* 103 (2003) 1–31.
- [34] S. Asakura, F. Oosawa, On interaction between 2 bodies immersed in a solution of macromolecules, *J. Chem. Phys.* 22 (1954) 1255–1256.
- [35] J. Taffs, A. Malins, S.R. Williams, C.P. Royall, A structural comparison of models of colloid–polymer mixtures, *J. Phys., Condens. Matter* 22 (2010) 104119.
- [36] M.P. Allen, D.J. Tildesley, *Computer Simulation of Liquids*, Oxford University Press, Oxford, UK, 1989.
- [37] S.R. Williams, Topological classification of clusters in condensed phases, arXiv: 0705.0203v1 [cond-mat.soft] (2007).

- [38] N.J.A. Sloane, R.H. Hardin, J.H. Conway, Minimal energy clusters of hard spheres, *Discrete Comput. Geom.* 14 (1995) 237–259.
- [39] J. Fornleitner, G. Kahl, Lane formation vs. cluster formation in two dimensional square-shoulder systems – a genetic algorithm approach, *Europhys. Lett.* 82 (2008) 18001.
- [40] A.J. Archer, N.B. Wilding, Phase behavior of a fluid with competing attractive and repulsive interactions, *Phys. Rev. E.* 76 (2007) 031501.
- [41] M. Tarzia, A. Coniglio, Pattern formation and glassy phase in the ϕ^4 theory with a screened electrostatic repulsion, *Phys. Rev. Lett.* 96 (2006) 075702.
- [42] C.P. Royall, S.R. Williams, T. Ohtsuka, H. Tanaka, Direct observation of a local structural mechanism for dynamic arrest, *Nat. Mater.* 7 (2008) 556–561.
- [43] P.J. Lu, E. Zaccarelli, F. Ciulla, A.B. Schofield, F. Sciortino, D.A. Weitz, Gelation of particles with short-range attraction, *Nature* 435 (2008) 499–504.